

Catalytic activity of Pt–Au/CeO₂ catalyst for the preferential oxidation of CO in H₂-rich stream

Sutarawadee Monyanon^a, Sangobtip Pongstabodee^a, Apanee Luengnaruemitchai^{b,*}

^a Department of Chemical Technology, Chulalongkorn University, Bangkok 10330, Thailand

^b The Petroleum and Petrochemical College, Chulalongkorn University, Bangkok 10330, Thailand

Received 4 August 2006; received in revised form 19 September 2006; accepted 19 September 2006

Available online 1 November 2006

Abstract

We have investigated the relationship between the catalyst preparation and the catalytic activity of Pt–Au/CeO₂, Pt/CeO₂ and Au/CeO₂ catalysts for preferential oxidation (PROX) of CO in simulated reformed gas. The prepared catalysts were characterized by XRD, XRF, BET, SEM, TEM and TPR techniques. The catalytic activity tests were carried out in the temperature range of 50–190 °C under atmospheric pressure. The results indicated that all single-step sol–gel catalysts exhibited the maximum CO conversion. The amount of metal loading and the ratios of Pt–Au catalysts had an important effect on the catalytic activity. In addition, the blockage of catalytic active sites by adsorbed H₂O and CO₂ in the feed stream decreased the activity of the Pt–Au/CeO₂ catalysts. This catalyst exhibited good stability.

© 2006 Elsevier B.V. All rights reserved.

Keywords: Pt–Au; Cerium oxide; Preferential oxidation of CO

1. Introduction

Proton exchange membrane fuel cells (PEMFC) have largely been studied due to their high-energy conversion efficiency [1,2]. In general, the hydrogen produced by the steam reforming or partial oxidation of hydrocarbons or liquid fuels followed by water-gas shift reaction contains about 1 vol.% CO. Unfortunately, a small amount of CO, which is poisoning agent, has a negative effect on PEMFC electrodes, which are typically made of Pt. Among the CO removing methods, the preferential oxidation (PROX) of CO seems to be the simplest and the least expensive method [3]. However, in this reaction water is formed via hydrogen oxidation, reverse water gas shift and CO-methanisation reactions. The side reactions are as follows:



Supported noble metal catalysts (Pt, Rh, Ru, Pd, Ir) have been effective for the PROX of CO. Especially, Pt is very active and stable for CO removal and minimal loss of H₂ at high temperatures (in the temperature range of 175–200 °C) [3–5]. Our previous works [6,7] demonstrated the activity of Au for this reaction. Moreover, at low temperatures, highly dispersed Au on an appropriate oxide support showed high activity and selectivity [8,9]. An Au catalyst is inert for catalytic applications, however, it is more active for selective CO oxidation [10–12], and more for CO oxidation than for H₂ oxidation [13]. In addition, the catalytic activity of Au is enhanced by moisture and is almost insensitive to CO₂ [14,15]. However, it has been reported that the catalytic performance strongly depends on the catalyst preparation.

For the supports, mostly metal oxides, ceria is an interesting one because of its unique redox properties and high oxygen storage capacity. The oxygen mobility in the crystallographic structure, therefore, is greatly facilitated. Moreover, it has been reported that it can promote water-gas shift activity, maintain the dispersion of the catalytic metals and stabilize the surface area of the support [16–18].

To develop the PEMFC applications, it is necessary to explore catalysts that can be used at low temperatures and in the presence of CO₂ and H₂O. Among the catalysts studied, supported

* Corresponding author. Tel.: +66 2 218 4148; fax: +66 2 215 4459.
E-mail address: apanee.l@chula.ac.th (A. Luengnaruemitchai).

Pt catalysts have a high CO conversion at high temperatures, but the activity is decreased at low temperatures. Besides the Pt catalyst, the use of an oxide-supported Au catalyst is essential for the improvement of the selectivity at low temperatures for the CO oxidation. In addition, bimetallic nanoparticles are of wide interest since they lead to many interesting properties, and the study of Pt–Au catalysts has afforded the opportunity to study the importance of geometric effects on the catalysis by Pt. Bulk and supported Pt–Au alloys have been extensively studied as catalysts for the reactions of alkanes and cycloalkanes [19,20]. Therefore, in this work we have investigated and carried out comparative catalytic studies on PtAu/CeO₂ prepared by different methods for the selective CO oxidation reaction with Pt/CeO₂ and Au/CeO₂ catalysts. Here, we present the effects of preparation method on Pt–Au supported on CeO₂ catalysts, Pt:Au ratios, total metal loading, and the optimum operating conditions on the catalytic activity for the PROX of CO in the presence of H₂. Additionally, the prepared catalysts were also investigated in the presence of CO₂ and H₂O and stability tests were done.

2. Experimental

2.1. Support preparation

The support was prepared by sol–gel method [21]. Two solutions of Ce(NO₃)₃·6H₂O (Merck) and urea (Asia Pacific Specialty Chemicals Limited) were prepared by mixing 0.1 M of Ce(NO₃)₃·6H₂O with 0.4 M of the urea solution. The solution was aged at 100 °C for 50 h. Then, the precipitate was washed with deionized water and ethanol. The support was dried overnight at 110 °C and calcined at 300 °C for 2 h in air.

2.2. Catalyst preparation

The catalysts were prepared by two methods:

- **Impregnation.** The catalysts were obtained by co-impregnating the appropriate amount of an aqueous solution of HAuCl₄·3H₂O and H₂PtCl₆·6H₂O (Fluka) onto the commercial and synthesized ceria supports. The catalysts were then dried overnight at 110 °C and calcined at 500 °C for 5 h.

- **Single-step sol–gel.** The catalysts were prepared from the aqueous solution of HAuCl₄·3H₂O and H₂PtCl₆·6H₂O in an aqueous mixture of Ce(NO₃)₃·6H₂O and urea. The mixture was aged at 100 °C for 50 h and the precipitate was then washed with deionized water and ethanol many times. The catalysts were dried overnight at 110 °C and calcined at 500 °C for 5 h.

2.3. Catalyst characterization

A Rigaku X-ray diffractometer (XRD) system equipped with a RINT 2000 wide-angle goniometer using Cu K α radiation and a power of 40 kV \times 30 mA was used for the examination of the crystalline structure. X-ray fluorescence spectroscopy (XRF) was used for the analysis of all the elements. The Brunauer–Emmett–Teller (BET) method, using a Quantachrome Corporation Autosorb, was used to determine the surface area and pore size of the prepared catalyst by N₂ adsorption/desorption at –196 °C. Prior to the analysis, the samples were outgassed at 250 °C for 2 h.

Transmission electron microscope (TEM) and scanning electron microscope (SEM) images were used to obtain information about the morphology and crystal structures of the catalysts. Temperature programmed reduction (TPR) was used to investigate the reduction temperatures of the catalysts.

2.4. Catalytic activity

Catalytic activity was carried out in a U-tube reactor (i.d. 6 mm) mounted in the constant temperature zone of an electric furnace. A sample of 100 mg was packed between two layers of glass wool. Prior to reaction, the catalysts were treated in H₂ at 400 °C for 2 h. The catalytic activity was investigated in the temperature range of 50–190 °C. The feed stream contained 40% H₂, 1% CO, 1% O₂, 0–10% H₂O and 0–25% CO₂ (He balance) at a total flow rate of 50 ml min^{–1} (SV = 30,000 ml g^{–1} h^{–1}) under atmospheric pressure. The effluent gas was detected by an on-line gas chromatograph (Agilent Technologies 6890N model) equipped with a carbosphere column and a thermal conductivity detector (TCD). The CO conversion was based on the carbon dioxide formation. The CO selectivity was defined as the ratio of O₂ consumption for the CO oxidation over the total O₂ consumption.

Table 1
Characteristics of the prepared catalysts

Catalyst	Preparation method	BET surface area (m ² g ^{–1})	Ceria crystallite size ^a (nm)
CeO ₂	Commercial (as received)	12.27	53.53
CeO ₂	Sol–gel	116.78	16.18
1% Pt–Au/CeO ₂	Impregnation on commercial ceria	12.57	34.86
1% Pt–Au/CeO ₂	Impregnation on sol–gel ceria	111.90	16.58
1% Pt–Au/CeO ₂	Single-step sol–gel	83.92	15.14
0.5% Pt–Au/CeO ₂	Single-step sol–gel	–	30.77
2% Pt–Au/CeO ₂	Single-step sol–gel	–	21.15
1% Pt/CeO ₂	Single-step sol–gel	95.59	13.65
1% Au/CeO ₂	Single-step sol–gel	79.28	13.64

^a Estimated by XRD.

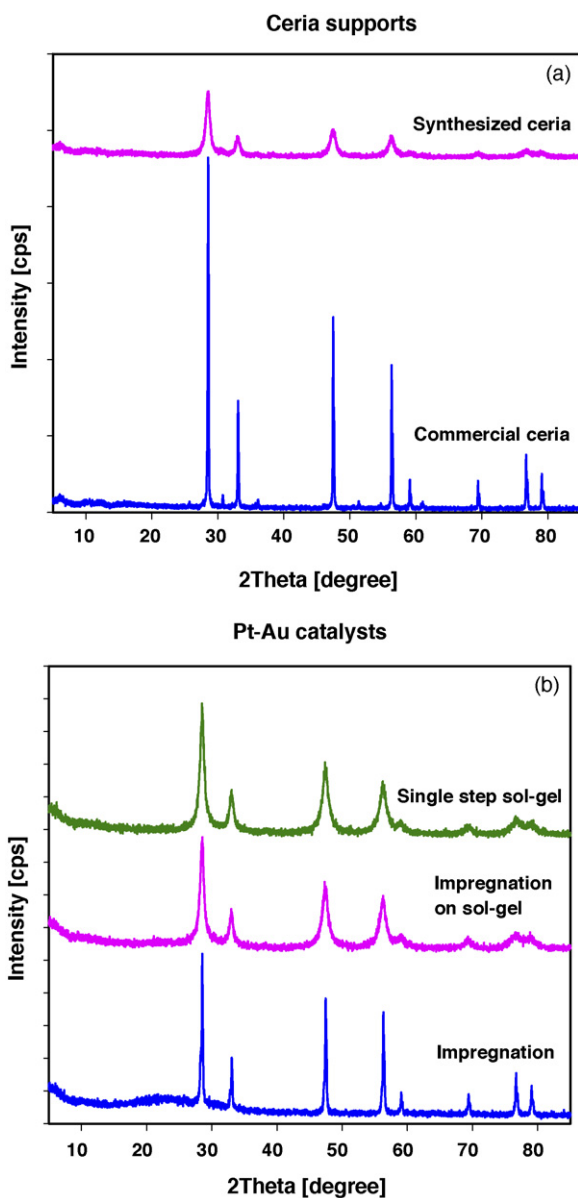


Fig. 1. XRD patterns of (a) ceria support and (b) 1% (1:1)PtAu/CeO₂ catalyst.

3. Results and discussion

3.1. Catalyst characterization

The specific surface areas and CeO₂ crystallite size results are summarized in Table 1. It shows that the catalyst preparation method affected the surface area of the prepared catalysts. The commercial ceria support has a surface area less than the synthesized ceria, while the catalysts prepared by single-step sol-gel did not show much difference in the range of 79.28–95.29 m² g⁻¹. The CeO₂ crystallite sizes of the catalysts were determined from X-ray line-broadening using the Debye-Scherrer equation. The sol-gel method seems to be better than impregnation because of the higher surface area and smaller ceria crystallite size. It is obvious that the ceria crystallite size depends on the support of the catalyst.

The XRD patterns of 1% (1:1)PtAu/CeO₂ catalysts in Fig. 1b shows the typical patterns of the CeO₂ (Fig. 1a) and no metal peaks were found, indicating that the metallic particle size of the prepared catalysts is either atomically dispersed or too small to be detected by XRD methods, which were similar to those of 1% Pt/CeO₂ and 1% Au/CeO₂ catalysts (not shown in this paper). A difference in peak intensity may originate from the different degrees of crystallinity of CeO₂.

The SEM images of the two supports, commercial ceria and the synthesized ceria, and 1% (1:1)PtAu/CeO₂ catalyst prepared by sol-gel are given in Fig. 2. The SEM results of the supports are confirmed by XRD results, which show that the crystallinity of the commercial ceria is higher than that of the synthesized ceria. The particles of synthesized ceria are mainly of long thin crystal shaped morphology. A similar SEM result of synthesized CeO₂ was reported elsewhere [22].

TEM was applied to ascertain the crystallinity and the size of metals in these catalysts. Fig. 3 shows the TEM images of the 1% (1:1)PtAu/CeO₂ catalysts prepared by sol-gel. The size of the contrasted particles measured from TEM ranged between 5 and 10 nm.

TPR patterns of the monometallic catalysts (1% Pt/CeO₂ and 1% Au/CeO₂) and the bimetallic catalyst (1% (1:1)PtAu/CeO₂) prepared by single-step sol-gel are shown in Fig. 4. The TPR pattern of Au/CeO₂ shows a broadened peak situated close to ~400 °C. The TPR profile of PtAu/CeO₂ catalysts is significantly different from either of the monometallic profiles. They

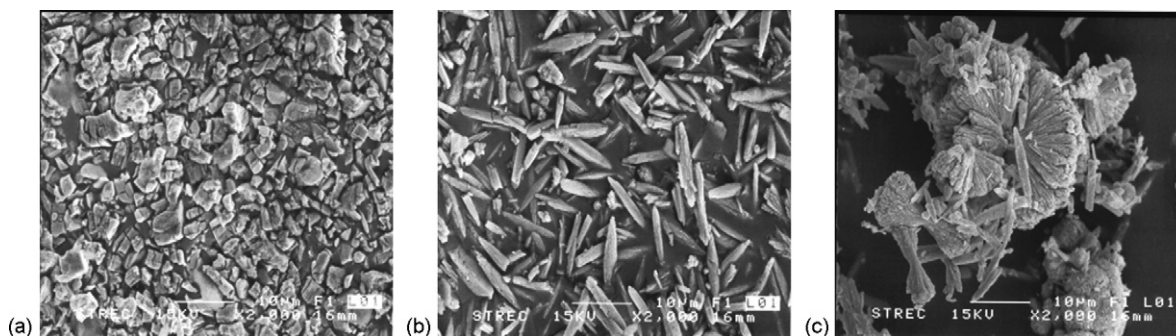


Fig. 2. SEM images of (a) commercial ceria, (b) synthesized ceria and (c) 1% (1:1)PtAu/CeO₂ catalyst.

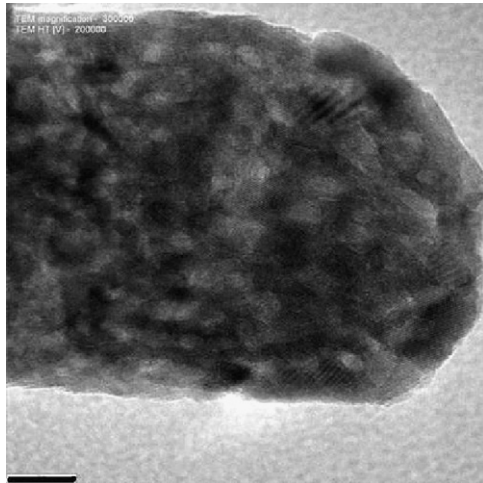


Fig. 3. TEM image of 1% (1:1)PtAu/CeO₂ catalyst.

also reveal a significant lowering of the reduction temperature of 1% PtAu/CeO₂ when compared to Au/CeO₂, which implies that the Pt and Au interact strongly and help to weaken the surface oxygen on the ceria thereby improving the reducibility of the catalyst. This interaction may form a new phase, which shows a lower reduction temperature. The results are in good agreement with Suh et al. and show that the excellent performance of the bimetallic catalyst is due to the formation of a new phase, which may be more active for the selective oxidation of CO than Pt/Al₂O₃.

3.2. Catalytic activity

3.2.1. Effect of catalyst preparation method

Fig. 5 compares the catalytic performance in terms of CO conversion and selectivity of 1% Pt/CeO₂, 1% Au/CeO₂ and 1% (1:1)PtAu/CeO₂ catalysts versus reaction temperature for dry gas composition of 1% CO, 1% O₂, 40% H₂, and a He

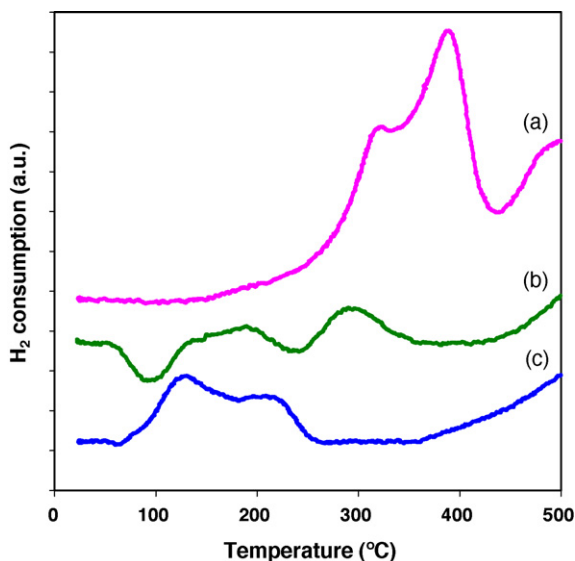


Fig. 4. TPR patterns of (a) 1% Au/CeO₂, (b) 1% Pt/CeO₂ and (c) 1% (1:1)PtAu/CeO₂.

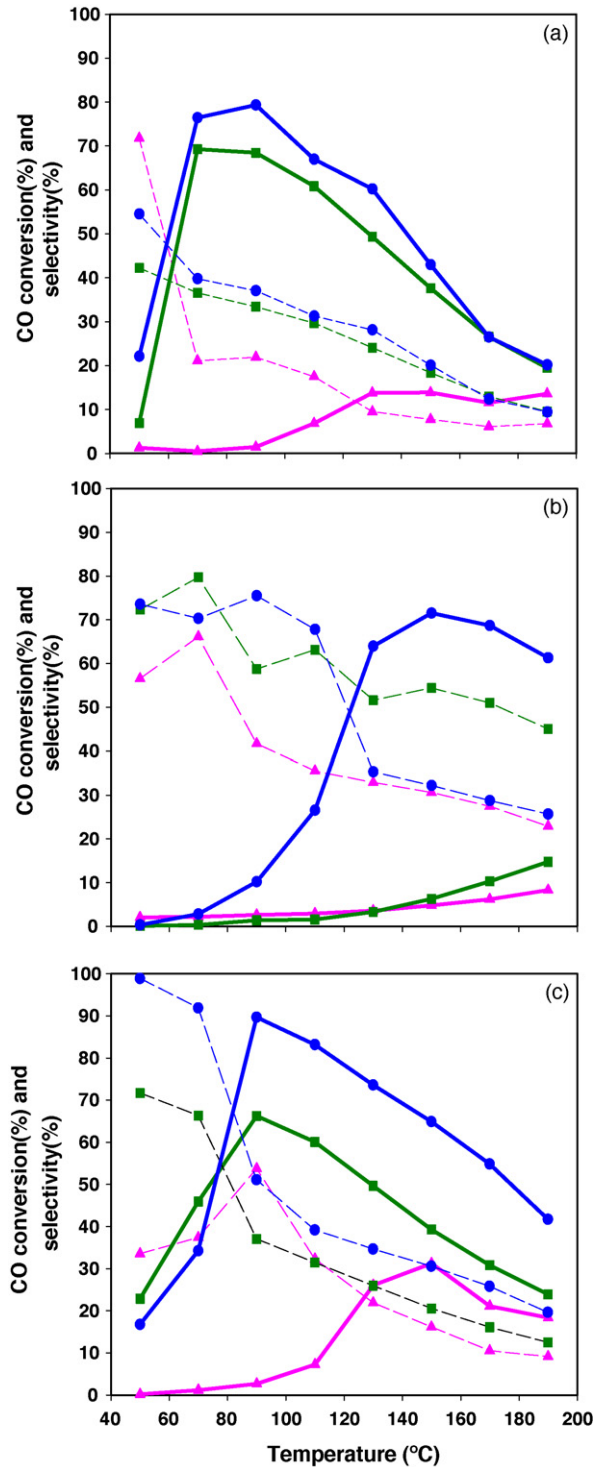


Fig. 5. Temperature dependence of (a) 1% Pt/CeO₂, (b) 1% Au/CeO₂ and (c) 1% (1:1)PtAu/CeO₂ catalysts. Reactant composition: 1% CO, 1% O₂, 40% H₂ in He balance: (▲) impregnation; (■) impregnation on sol-gel; (●) single-step sol-gel; (—) CO conversion; (---) selectivity.

balance. The results showed a similar behavior in that the activity of all catalysts increased with increasing temperatures at the low temperature range. At high temperatures, the rate of H₂ oxidation is higher than that of CO oxidation; therefore, the conversion and selectivity was decreased. The behavior of the conversion and

selectivity are in agreement with our previous studies. These suggested that single-step sol–gel catalysts exhibited the best performance among the catalysts prepared by the three methods of catalyst preparation.

At low temperatures, as indicated in Fig. 5, the selectivity for CO oxidation on Au catalysts is ~ 70 – 80% (Fig. 5b), whereas Pt shows a significantly lower selectivity (~ 40 – 50%) (Fig. 5a). We have shown that at low-temperatures, the PtAu catalyst should be more selective than the Pt catalyst.

The maximum CO conversions are $\sim 80\%$ (at 80°C), $\sim 70\%$ (at 150°C) and $\sim 90\%$ (at 90°C) for 1% Pt/CeO₂, 1% Au/CeO₂ and 1% (1:1)PtAu/CeO₂ catalysts, respectively. There is much literature showing that the influence of preparation method has a strong effect on the activity of catalysts. Compared to the other methods, the single-step sol–gel method gave the smallest ceria crystallite size (15.14 nm), investigated by XRD, as shown in Table 1. Moreover, the TEM result seems to reveal that the interface between active metals and support is homogeneous, resulting in a strong interaction. In our previous work, Parinyasawan et al. [23] found that 1% (1:7)PtPd/CeO₂ prepared by impregnation on sol–gel exhibited the maximum activity of $\sim 75\%$ CO conversion and $\sim 55\%$ selectivity at 90°C , which is attributed to the highest dispersion of active metals on the ceria surface, compared to other examined catalysts. Haruta et al. [24,25] illustrated that Au nanoparticles on metal oxides prepared by co-precipitation and deposition-precipitation methods exhibit surprisingly high catalytic activity for CO oxidation. For Pt catalysts, Manasilp and Gulari [26] used the single-step sol–gel method to prepare Pt/Al₂O₃ catalysts due to their high surface area and appears to have more interactions between the metal crystallite and the support, based on the observed resistance to sintering. Furthermore, Wu et al. [27] prepared Pt-doped ceria–zirconia solid solution (Ce_{0.66}Zr_{0.32}Pt_{0.22}O₂) synthesized by sol–gel method. Part of the Pt is introduced into the ceria lattice and shows higher oxygen mobility in the ceria–zirconia solid solution, larger reducibility of the noble metal, and better thermal stability.

A comparison between the catalytic activity of monometallic (1% Pt/CeO₂, 1% Au/CeO₂) and bimetallic (1% (1:1)PtAu/CeO₂) catalysts prepared by single-step sol–gel in the presence of a large amount of hydrogen (40% H₂, 1% CO, and 1% O₂ with He as a balance) is shown in Fig. 5. We found that the bimetallic prepared by single-step sol–gel has better performance than that of the monometallic. These results obtained with the bimetallic catalyst were similar to those observed by Suh et al. They found that the addition of base metal into the Pt catalyst enhanced the catalytic performance. Moreover, Zhang et al. [28] indicated that the addition Pt into Au/ZnO improved its stability during the test. In this work, Au/CeO₂ readily reached maximum conversion and selectivity at $\sim 70\%$ and $\sim 35\%$, respectively, at the higher temperature, 150°C . As a comparison, the maximum activity at 90°C of the Pt/CeO₂ catalyst is much higher than that of Au/CeO₂. The presence of Au in the PtAu/CeO₂ catalyst causes $\sim 90\%$ conversion at 90°C , which is relatively high compared to the 80% conversion of the Pt/CeO₂ catalyst. For the selectivity, PtAu/CeO₂ showed the highest values of all at about 70 – 90% in the range of 50 – 80°C . Therefore, these results

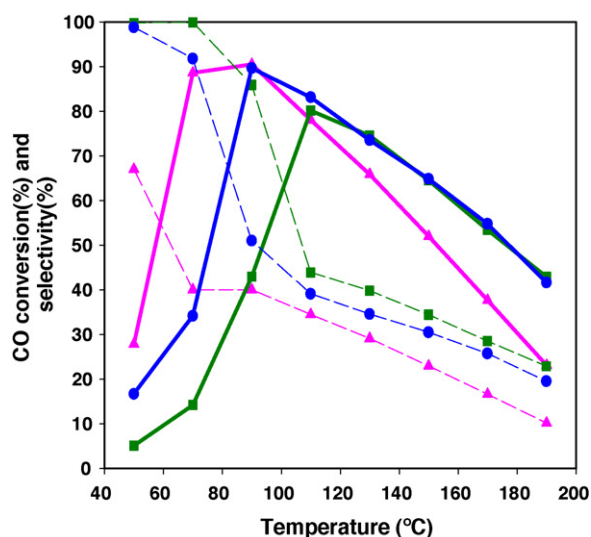


Fig. 6. Effect of Pt:Au ratios over 1% PtAu/CeO₂ single-step sol–gel catalyst. Reactant composition: 1% CO, 1% O₂, 40% H₂ in He balance: (▲) 10:1 ratio; (●) 1:1 ratio; (■) 0.2:1 ratio; (—) CO conversion; (---) selectivity.

demonstrated that the bimetallic catalyst has the highest activity in the low temperature range.

3.2.2. Effect of Pt:Au ratio (1% metal loading)

Fig. 6 shows the activity of the selective CO oxidation of 1% PtAu/CeO₂ catalyst with various ratios of Pt and Au, which are 10:1, 1:1 and 0.2:1, as a function of reaction temperature. It indicates that the activity was increased with increasing Pt content and the maximum CO conversion also shifted to lower temperature. However, the selectivity of PtAu/CeO₂ (10:1) at the maximum CO conversion (at ~ 70 – 90°C) is the lowest value compared to the others. As a consequence, a 1:1 Pt:Au ratio gave the best performance ($\sim 90\%$ CO conversion and $\sim 40\%$ selectivity) at 90°C . This may contribute to the highest dispersion of this catalyst. In addition, Pt and Au were found to be homogeneous and well dispersed on the support material, as there is evidence of its presence in either EDS or TEM. This agrees very well with our previous study with the PtPd/CeO₂ catalyst, at a ratio of Pt:Pt = 1:7 with the highest metal dispersion showing the highest activity at the range of 90 – 110°C . Zhang et al. studied the addition of Pt into Au/ZnO catalyst and found that the ratio of Pt to Au is 1:1.5 gave the highest activity in their work.

3.2.3. Effect of total metal loading

A series of PtAu/CeO₂ catalysts was prepared with different total metal loadings (0.5, 1, 2 wt.%) at a Pt:Au ratio of 1:1. Fig. 7 shows CO conversion and selectivity as a function of temperature of the PtAu/CeO₂ catalysts. From the trends for the CO conversion, it is seen that the CO conversion did not show much difference while the selectivity of 1 wt.% metal loading is the highest of all at low temperatures. It is clear that the activity is directly related to the CeO₂ crystallite sizes (Table 1). The average CeO₂ crystallite sizes are 30.77, 15.14 and 21.15 nm, for 0.5, 1 and 2 wt.%, respectively, which is affected by the degree of metal dispersion on the catalyst support.

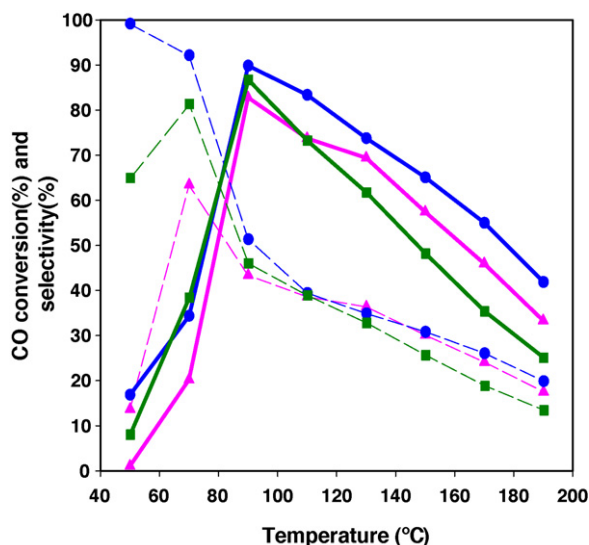


Fig. 7. Effect of % total metal loading over 1% (1:1)PtAu/CeO₂ single-step sol-gel catalyst. Reactant composition: 1% CO, 1% O₂, 40% H₂ in He balance: (▲) 0.5%; (●) 1%; (■) 2%; (—) CO conversion; (---) selectivity.

3.2.4. Effect of CO₂

The effect of the CO₂ addition to the feed stream of the 1% (1:1)PtAu/CeO₂ catalyst prepared by single-step sol-gel is shown in Fig. 8. The result shows that the maximum CO conversion dropped from ~90% to ~65% with a shift of 20 °C to higher temperatures. However, when the CO₂ concentration is increased from 5% to 25%, there is slightly decreased CO conversion. For the selectivity, there is a decrease with increasing concentration of CO₂ in the low temperature range, but at higher temperature there is a minimum loss of selectivity. The explanation for these differences in catalytic behavior upon the addition of CO₂ is unclear so far. The effects of CO₂ on the selective CO oxidation reaction have been studied for a variety

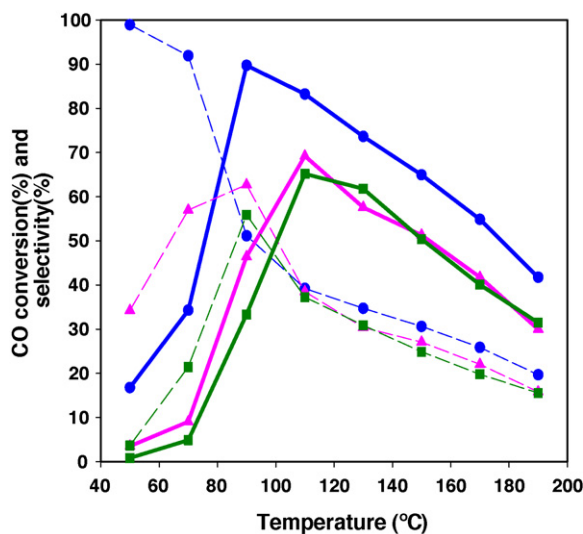


Fig. 8. Effect of CO₂ in the feed stream over 1% (1:1)PtAu/CeO₂ single-step sol-gel catalyst. Reactant composition: 1% CO, 1% O₂, 0–25% CO₂, 40% H₂ in He balance: (●) 0% CO₂; (▲) 5% CO₂; (■) 25% CO₂; (—) CO conversion; (---) selectivity.

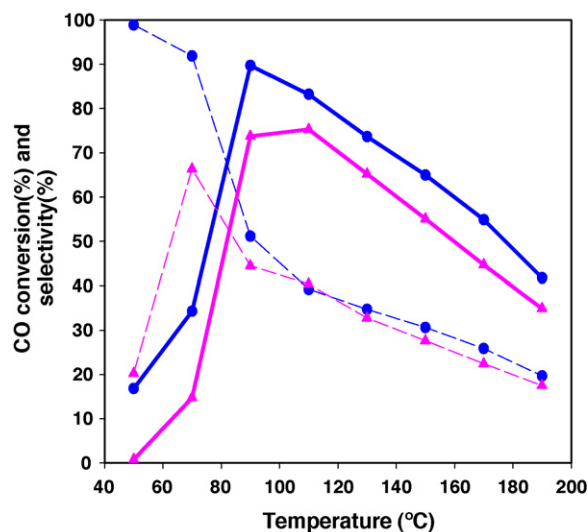


Fig. 9. Effect of H₂O in the feed stream over 1% (1:1)PtAu/CeO₂ single-step sol-gel catalyst. Reactant composition: 1% CO, 1% O₂, 0–10% H₂O, 40% H₂ in He balance: (●) 0% H₂O; (▲) 10% H₂O; (—) conversion; (---) selectivity.

of supported Au catalysts and both positive and negative effects were reported. In contrast to Au catalysts, the effects of CO₂ on supported Pt catalysts have rarely been studied. Our finding of a decrease in activity in the presence of CO₂ in the feed stream agrees well with the studies of Panzera et al. and Schubert et al. [29]. They found that deactivation is accelerated due to increased carbonate formation, which competes with CO adsorption on the catalyst surface. It has also been reported that it is caused by the reverse water gas reaction.

3.2.5. Effect of water vapor

The effect of the presence of water vapor in the feed is shown in Fig. 9. The results obtained over the 1% PtAu/CeO₂ catalyst showed that the presence of water vapor in the feed stream provokes a significant decrease in CO conversion. However, the addition of water had a slightly negative effect on the CO oxidation rate compared to the effect of CO₂. The addition of 10% H₂O into the feed decreases the activity of 1% PtAu/CeO₂ from ~90% to ~75% CO conversions at 90 °C. Its maximum CO conversion temperature remains similar; it is likely that the temperature dependence turns out to be less pronounced. Compared to the dramatic decrease in CO oxidation, the changes observed in selectivity show insignificant impact at high temperatures. The presence of water has decreased the selectivity by ~3% over the range of 110–190 °C. This may be due to the blocking of water on the active sites, which was reported by Daté et al. [30]. In contrast to PtPd/CeO₂ [23], it was found that a considerable increase in CO conversion and selectivity was observed over the entire temperature range investigated (~50–190 °C) upon addition of water (~10% H₂O).

3.2.6. Effect of CO₂ and H₂O

We also investigated the influence of co-added 25% CO₂ and 10% water vapor in the feed stream on the selective CO oxidation over 1% (1:1)PtAu/CeO₂ catalyst as shown in Fig. 10. It was found that the activity is clearly diminished due to the carbonate

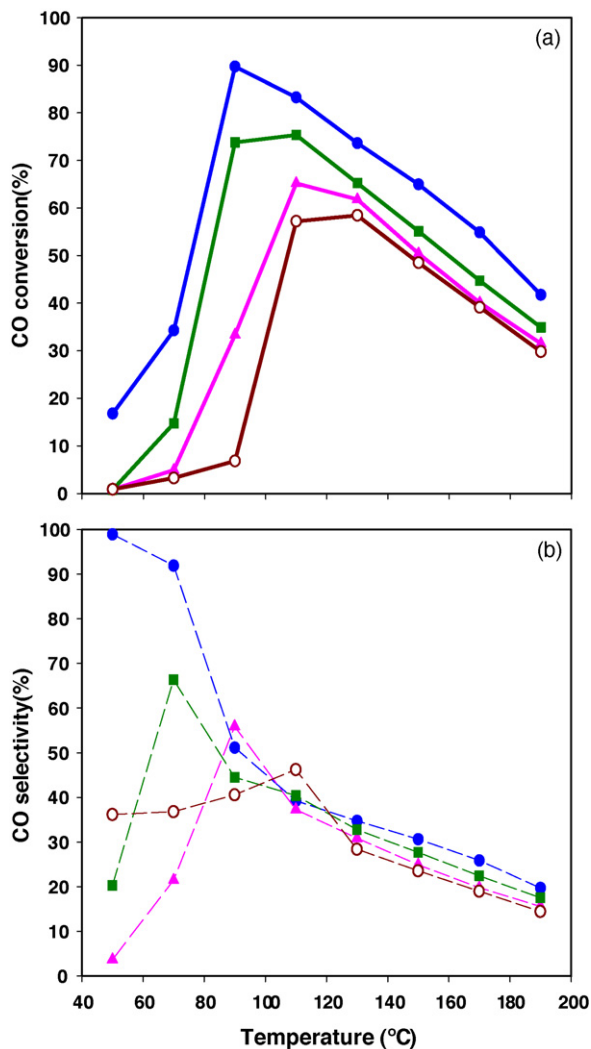


Fig. 10. Effects of CO₂ and H₂O concentration in the feed stream over 1% (1:1)PtAu/CeO₂ single-step sol-gel catalyst. Reactant composition: 1% CO, 1% O₂, 0–10% H₂O, 0–25% CO₂, 40% H₂ in He balance: (●) 0% CO₂ + 0% H₂O; (▲) 25% CO₂ + 0% H₂O; (■) 0% CO₂ + 10% H₂O; (○) 25% CO₂ + 10% H₂O; (—) CO conversion; (---) selectivity.

species and water vapors competing for adsorption with CO on the active sites, which is in agreement with Schubert et al. It is apparent that the temperature at maximum CO conversion also shifts to higher temperatures when both CO₂ and H₂O are present. It could be explained that the main cause for the negative effect of CO₂ and H₂O in the feed may be attributed to the competitive adsorption of CO and CO₂ as well as the blockage of the active sites by water vapor. However, at high temperatures (>110 °C), the selectivity of PtAu/CeO₂ does not change much.

3.2.7. Deactivation test

To further evaluate the stability of the catalyst, the 1% (1:1)PtAu/CeO₂ single-step sol-gel catalyst was tested at a temperature of 90 °C for 13 h, as shown in Fig. 11. The CO conversion and selectivity were maintained during the deactivation test with a very slight loss, although the spent catalyst has larger ceria crystallite size (~15.81 nm) than the fresh catalyst (~15.14 nm). We speculate that this result may be strongly

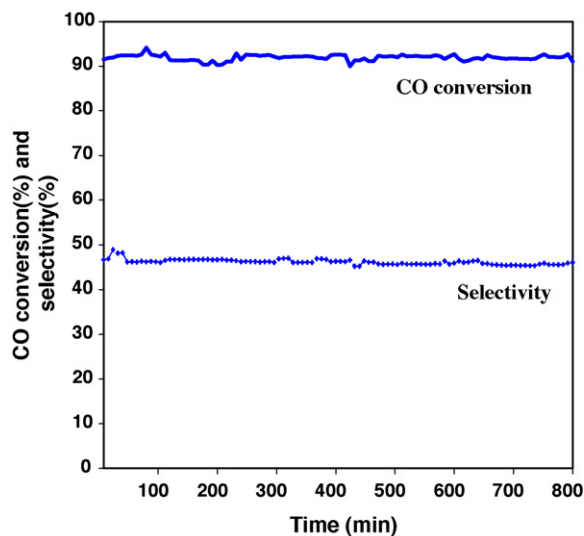


Fig. 11. Deactivation test over 1% (1:1)PtAu/CeO₂ single-step sol-gel catalyst. Reactant composition: 1% CO, 1% O₂, 40% H₂ in He balance: (—) CO conversion; (---) selectivity.

affected by the preparation method since there appears to be more interaction between the support and the metal.

4. Conclusions

In this study, we can make conclusions about the catalytic activity of a series of PtAu/CeO₂ catalysts for PROX of CO in the temperature range of 50–190 °C as follows.

The bimetallic catalysts (PtAu/CeO₂) are more active than monometallic catalysts (Pt/CeO₂, Au/CeO₂) and their activities are between the activities of monometallic catalysts, exhibiting high activity at 90 °C. The catalysts prepared by the single-step sol-gel method, using urea as the hydrolysis agent and pretreated by H₂, gave the best performance, and this method gives the smallest ceria crystallite size and strong interaction between active metals and support. Among the PtAu/CeO₂ catalysts with different Pt: Au ratios and total metal loadings, the 1% PtAu(1:1)/CeO₂ catalyst exhibits the best catalytic performance.

When both CO₂ and water vapor are added to the feed stream, the activity of the catalyst is significantly impacted with lower activity. However, the activity of this catalyst could not achieve the low CO-acceptable level for PEMFC applications. Further work must be performed to achieve the CO-acceptable level and CO selectivity such as two-stage PROX reactor.

Acknowledgments

This work was partially supported by the Postgraduate Education and Research Programs in the Department of Chemical Technology and The Petroleum and Petrochemical College, Chulalongkorn University, Thailand. The Thailand Research Fund (TRF) is also acknowledged for financially supporting this work.

References

- [1] A.J. Appleby, F.R. Foulkes, *Fuel Cell Handbook*, Van Nostrand Reinhold, New York, 1990, pp. 15–26.
- [2] J. Larmanies, A. Dicks, *Fuel Cell Systems Explained*, Wiley, Chichester, New York, 2000, pp. 38–53.
- [3] F. Mariño, C. Descorme, D. Duprez, *Appl. Catal. B: Environ.* 54 (2004) 59–66.
- [4] D.J. Suh, C. Kwak, J.-H. Kim, S.M. Kwon, T.-J. Park, *J. Power Sources* 142 (2005) 70–74.
- [5] S.H. Oh, R.M. Sinkevitch, *J. Catal.* 142 (1993) 254–262.
- [6] A. Luengnaruemitchai, S. Osuwan, E. Gulari, *Int. J. Hydrogen Energy* 29 (2004) 429–435.
- [7] A. Luengnaruemitchai, S. Osuwan, E. Gulari, *Catal. Commun.* 4 (2003) 215–221.
- [8] G. Panzera, V. Modafferi, S. Candamano, A. Dotano, F. Frusteri, P.L. Antonucci, *J. Power Sources* 135 (2004) 177–183.
- [9] M. Haruta, N. Yamada, T. Kobayashi, M. Iijima, *J. Catal.* 115 (1989) 301–309.
- [10] J.-D. Grunwaldt, M. Maciejewski, O.S. Becker, P. Fabrizioli, A. Baiker, *J. Catal.* 186 (1999) 458–469.
- [11] F. Bocuzzi, A. Chiorino, M. Manzoli, P. Lu, T. Akita, S. Ichikawa, M. Haruta, *J. Catal.* 202 (2001) 256–267.
- [12] T.V. Choudhary, C. Sivadinarayana, C.C. Chusuei, A.K. Datye, J.P. Fackler Jr., D.W. Goodman, *J. Catal.* 207 (2002) 247–255.
- [13] M. Okumura, S. Tsubota, M. Haruta, *J. Mol. Catal. A: Chem.* 199 (2003) 73–84.
- [14] R.M.T. Sanchez, A. Ueda, K. Tanaka, M. Haruta, *J. Catal.* 168 (1997) 125–127.
- [15] W. Deng, J.D. Jesus, H. Saltsburg, M. Flytzani-Stephanopoulos, *Appl. Catal. B: Environ.* 291 (2005) 126–135.
- [16] J. Barbier Jr., D. Dopez, *Appl. Catal. B: Environ.* 4 (1994) 105–140.
- [17] A.F. Diwell, R.R. Rajaram, H.A. Shaw, T.J. Truex, *Stud. Surf. Sci. Catal.* 71 (1991) 139–148.
- [18] F. Mariño, C. Descorme, D. Duprez, *Appl. Catal. B: Environ.* 58 (2005) 175–183.
- [19] B.D. Chandler, L.I. Rubinstein, L.H. Pignolet, *J. Mol. Catal. A: Chem.* 133 (1998) 267–282.
- [20] J.K.A. Clarke, A.F. Kane, T. Baird, *J. Catal.* 64 (1980) 200–212.
- [21] K. Khumvilaisak, M.S. Thesis, *The Petroleum and Petrochemical College, Chulalongkorn University*, 2001. ISBN 974-13-0678-4.
- [22] M. Thammachart, V. Meeyoo, T. Risksomboon, S. Osuwan, *Catal. Today* 68 (2001) 53–61.
- [23] A. Parinyasawan, S. Pongstabodee, A. Luengnaruemitchai, *Int. J. Hydrogen Energy* 31 (2006) 1942–1949.
- [24] M. Haruta, M. Daté, *Appl. Catal. A: Gen.* 222 (2001) 427–437.
- [25] M. Haruta, S. Tsubota, T. Kobayashi, H. Kageyama, M.J. Genet, B. Delmon, *J. Catal.* 144 (1993) 175–192.
- [26] A. Manasilp, E. Gulari, *Appl. Catal. B: Environ.* 37 (2002) 17–25.
- [27] X. Wu, J. Fan, R. Ran, D. Weng, *Chem. Eng. J.* 109 (2005) 133–139.
- [28] J. Zhang, Y. Wang, B. Chen, C. Li, D. Wu, X. Wang, *Energy Convers. Manage.* 44 (2003) 1805–1815.
- [29] M.M. Schubert, A. Venugopal, M.J. Kalich, V. Plzak, R.J. Behm, *J. Catal.* 222 (2004) 32–40.
- [30] M. Daté, M. Haruta, *J. Catal.* 201 (2001) 221–224.